USING WEDM TO MACHINE A PURE MOLYBDENUM WELDING ELECTRODE

KATERINA MOURALOVA[1], RADIM ZAHRADNICEK[2]
RADIM HRDY[2]
[1]Brno University of Technology
Faculty of Mechanical Engineering
Brno, Czech Republic
[2]Brno University of Technology
Faculty of Electrical Engineering and Communication,
Brno, Czech Republic

e-mail: mouralova@fme.vutbr.cz

Materials and elements with a high melting point, including molybdenum, are suitable for high temperature physical applications and the fabrication of components such as welding electrodes or wires to be used in spark erosion wire-cut machines. The classic, or conventional, approaches to machining pure molybdenum are aptly complemented with the frequently used unconventional wire electrical discharge machining (WEDM) method. This paper proposes a detailed analysis of a WEDM-machined surface and its defects, as related to a welding electrode. Comprehensive information on the topography, including a 3D color-filtered representation of the surface, was acquired using a contact profiler and an atomic force microscope (AFM). The defects of the machined surfaces were examined with electron microscopy, both directly on the surface of a given sample and within its cross section. The entire set of associated processes also involved a local analysis of the chemical composition of the subsurface layer and a measurement of the relevant hardness.

1 INTRODUCTION

Wire electrical discharge machining (WEDM) is considered an unconventional method within the given subdomain of technology as the material is removed by continuously repeated electrical discharges. Such machining can be performed on any material that exhibits at least a minimum electrical conductivity, and no limit is defined in terms of the hardness or ductility of the workpieces. The machining tool, a wire electrode, is not in direct contact with the workpiece; this configuration excludes the action of mechanical forces and facilitates the high precision machining of delicate pieces, including thin-wall components. WEDM embodies a technique of major importance for multiple branches of industry, prominently including the automotive, aerospace, military, and medical fields [Mandal 2014], [Patel 2013], [Maher 2015]. The wide applicability of the procedure nevertheless carries with it ever-growing demands on the relevant performance characteristics, comprising, above all, the dimensional accuracy, material removal rate, and topography of the machined surface. These characteristics then depend on the type of the material being machined and its thermal treatment, operating condition of the machine, and selected parameters of the erosion process. Such parameters are then obtainable via various methods [Blecha 2011], [Blecha 2011].

The pure molybdenum electrode shown in Fig. 1 is utilized in the spot welding of brass sheets.
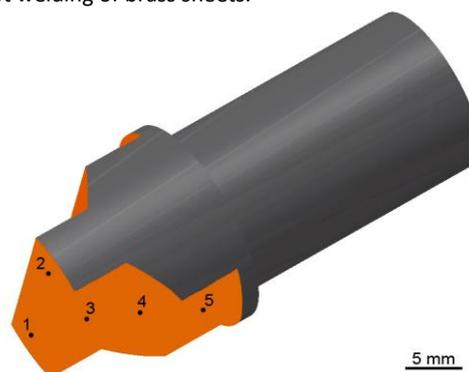
Figure 1. A model of the welding electrode, with the WEDM-machined surface and individual measurement points indicated in orange (The shape is not clearly displayed because of the company's conditions.).

2 EXPERIMENTAL SETUP AND MATERIAL

The experimental sample was manufactured from high purity (99.9) molybdenum, whose melting point of 2,623 °C enables it to be most frequently employed as an electrode material or a substrate for high temperature applications. In metallurgy, molybdenum finds use especially as a steel alloying agent to increase the strength and resistance to chlorine corrosion or mechanical wear. The metal element is also utilizable within the chemical industry, where it assumes the role of a catalyst or a lubricant (if combined with sulfur). The semi-product for this experiment exhibited the diameter of 20 mm.

The WEDM instrument used in the present study consisted in a high precision, five axis CNC machine MAKINO EU64. A pure copper wire with the diameter of 0.25 mm was employed as the electrode. The samples were immersed in deionized water, which embodied the dielectric medium and also removed the debris in the gap between the wire electrode and the workpiece during the process. The machine setting parameters, namely, the gap voltage, pulse on time, pulse off time, wire feed, and discharge current (Tab. 1), were all adjusted for copper with the thickness of 50 mm; the procedure was performed according to the instructions supplied by the manufacturer. Respecting these parameters, the real cutting speed corresponded to 0.6 mm/min.

Gap voltage (V)	Pulse on time (μs)	Pulse off time (μs)	Wire feed (m/min)	Discharge current (A)
40	8	66	16	22

Table 1. The machining parameters used in the experiment.

3 RESULTS OF THE EXPERIMENT AND DISCUSSION

The surface morphology, together with the areal and profile parameters of the machined area of the sample, was examined with a Bruker Dektak XT 3D contact profiler; the measured data were subsequently processed using Vision 64. We then utilized a Dimension Icon microscope (Bruker) to investigate the 3D topography of the surface of the sample, exploiting atomic-force microscopy (AFM); the obtained data were analyzed through the use of the Gwyddion software. The machined surface was also inspected with a Tescan LYRA3 scanning electron microscope (SEM), an instrument equipped with an energy-dispersion detector of X-rays (EDX) to facilitate the examination of WEDM-related changes in the chemical composition of the surface.
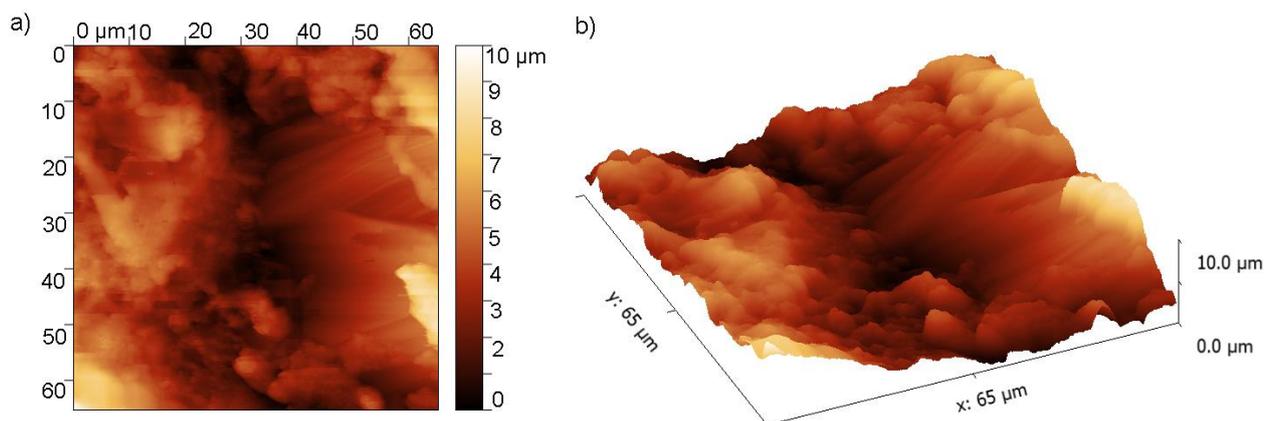
Figure 2. The 3D color-filtered images of the surface at location 2 on the sample.

In order to analyze the surface and subsurface microstructural changes and the variation in the chemical composition of the material machined via the WEDM method, we prepared metallographic specimens (cross-sections). The procedure was carried out via common methods, namely, wet grinding and polishing with diamond pastes, utilizing a Struers TEGRAMIN 30 automatic preparation device. The final mechanico-chemical polishing was conducted using the Struers OP-Chem suspension. After applying Hasson's tint etchant [Hasson 1968], we observed and documented the material structure by means of electron and light microscopy, employing a ZEISS Axio Observer Z1m inverted light microscope. The hardness measurement was then performed with a HYSITRON TI 950 TriboIndenter nanoindenter.

3.1 Surface evaluation: the profile and areal parameters; 3D topography

The Bruker Dektak XT 3D contact profiler, which detects the contact tip deflection due to the surface structure, enabled us to evaluate the profile parameters of the spark-eroded surface of the sample. The relevant parameters comprised the arithmetic mean deviation of profile (Ra), maximum height of profile (Rz), and root mean square deviation (Rq). The areal method was then used to evaluate the set of parameters incorporating the arithmetic mean height (Sa), maximum surface height (Sz), and root mean square height (Sq). In the wider context, the areal parameters facilitate the quantitative assessment of the surface in all technically significant respects (directions). Within the areal evaluation of surface quality, it is possible to set up the overall shape and general texture of the given surface in order to better predetermine its functional properties under operating conditions [Jiang 2012], [Waikar 2008], [Harcarik 2016].

The complete evaluation was performed via the Vision 64 software and in accordance with the standards related to areal [ISO 25178-2] and profile [ISO 4287] parameters. For the actual measurement, we selected 5 different locations on the surface of the sample, as shown in Fig. 1. The evaluated profile and areal parameters are presented in Tab. 2, exhibiting values comparable to those found in both the Ti-6Al-4V titanium alloy when thermally treated and the X210Cr12 hardened and tempered steel [Mouralova 2017].

The 3D topography of the machined surface was analyzed utilizing AFM, a semicontact technique to detect changes in the interaction forces between the tip and the workpiece surface occurring with variations of the distance of the tip from the surface. The measurement was conducted in the ScanAsyst

mode, with the applied tip having the radius of 0.65 μm and the assessed surface exhibiting the dimensions of 60x60 μm.

The detailed topography of the electroerosively machined surface is displayed in Fig. 2 above.

Place of measurement	Ra (μm)	Rq (μm)	Rz (μm)	Sa μm)	Sq (μm)	Sz μm)
1	2	2.4	10.4	2.3	2.4	12.5
2	2.2	2.8	14.1	2.6	2.9	14.8
3	2.2	2.7	11.4	2.5	2.9	12.3
4	2	2.6	13.3	2.3	2.7	15.1
5	2.7	3.2	15.9	2.9	3.5	16.7

Table 2. The areal and profile parameters evaluated at points 1 – 5 on the sample (according to Fig. 1).

3.2 Analyzing the surface morphology and chemical composition with the SEM and EDX techniques

The surface morphology of spark-machined pieces comprises multiple craters formed by individual electrical discharges that removed microscopic particles of the material; these particles were then washed away by a stream of dielectric fluid. Further material was eliminated from the cutting zone through temperatures as high as 10,000 – 20,000 °C [McGeough 1988]; such heat is typical of the discussed machining procedure. We investigated the surface of the welding electrode using electron microscopy, with the magnification rates of 1,000x; 2,500x; and 4,000x. The imaging was performed with a secondary electron (SE) and a backscattered electron (BSE) detectors.

Figure 3 below represents the morphology of the surface of a molybdenum electrode; here, the most important characteristic consists in marked cracks across the entire surface. Such cracks, visible without preparing a metallographic specimen, have hitherto not been studied in any other material. However, a substantially smaller form, or microcracks, was identified in Ti-6Al-4V titanium alloy [Aspinwall 2008] and pure titanium [Kumar 2013]. The analyzed surface morphology exhibits signs characteristic of a material entirely molten and subsequently rapidly cooled down; the surface comprises cracks generated by not only the volumetric changes due to phase transformations arising from the diffusion of both materials (the cut material and the cutting wire material) but also, and predominantly, the dilatation processes induced by very fast cooling (the melt transforming into a solid solution at an extremely high speed).
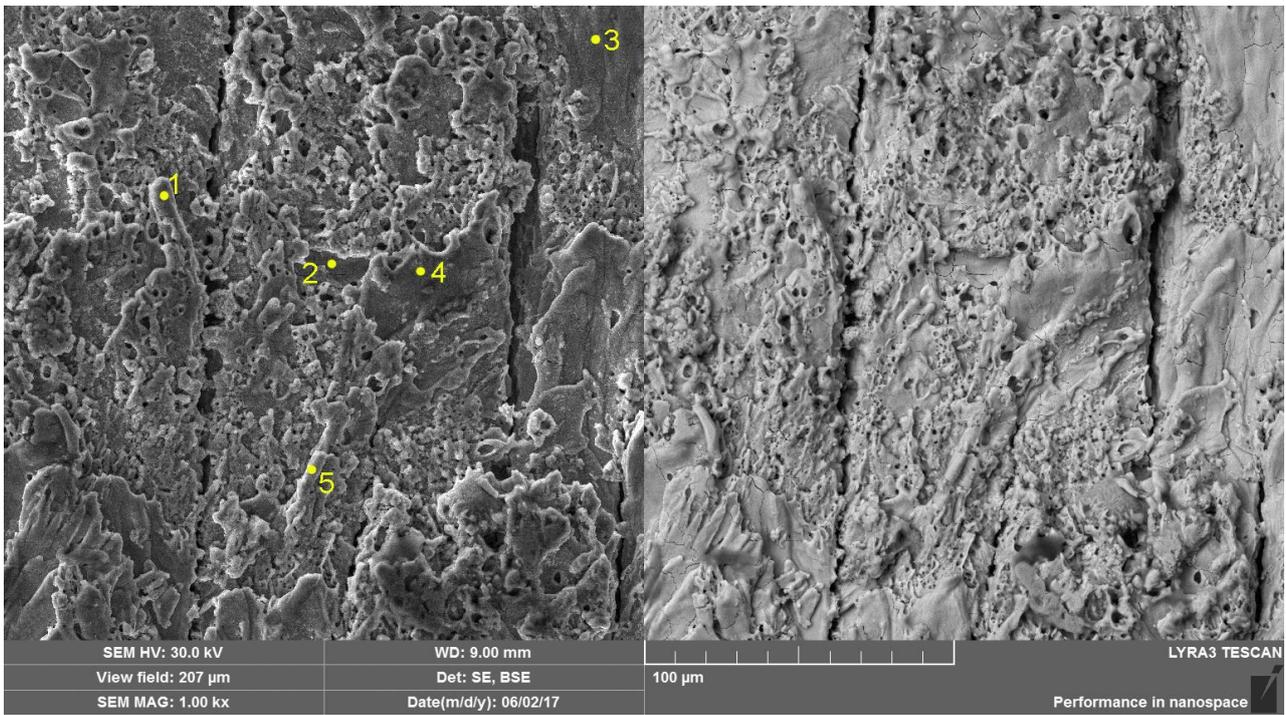
Figure 3. The morphology of the electrode surface, shown inclusive of the EDX (SEM) measurement spots (magnification rate: 1,000x).

The high temperatures result in very intensive diffusion processes between the wire electrode, made of brass in our case, and the machined material. Based on the data within Tab. 3, which presents the chemical composition at the individual measurement spots shown in Fig. 3, we can stress that the elements of the wire electrode (copper, zinc) and the machined material are mixed unevenly. Even though the wire electrode comprises 60% of copper and 40% of zinc, the diffusion does not respect this ratio, with the zinc diffused at a markedly lower rate. On the surface, a negligible quantity of carbon, likely produced through a contamination of the electron microscope chamber, was detected in all the points of measurement. The increased volume of oxygen at spots 2 and 4 is then explainable by the easy oxidability of molybdenum at elevated temperatures.

Figure 4. The chemical composition analysis, location 3 (as per Fig. 3).

Figure 4 displays the chemical analysis spectrum at location 3, where no elements of the wire electrode were found.

3.3 Analyzing the subsurface layers

In the metallographic specimens, the subsurface layer of a given sample was examined via light (objectives: 5x, 10x, 20x, 50x, and 100x) and electron microscopes, invariably with the magnification rates of 1,000x; 2,500x; and 4,000x, using backscattered electron detectors. The microstructure of the machined material, represented using light microscopy, is vividly shown in Fig. 5.

Place of measurement	Mo (wt.%)	C (wt.%)	O (wt.%)	Cu (wt.%)	Zn (wt.%)
1	89.5	2.4	2.1	5.8	0.2
2	79.2	2.7	12.5	5.5	0.1
3	89.7	3.3	7		
4	78.7	3.4	12.8	5.1	
5	87.9	2.5	6.9	2.7	

Table 3. The local chemical composition analysis (EDX), locations 1–5.
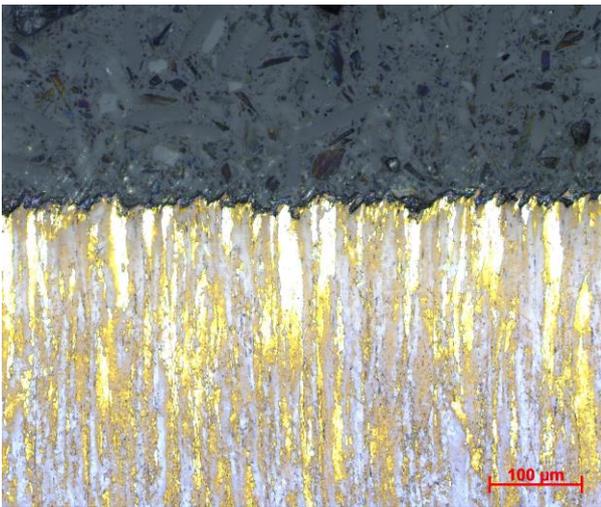
Figure 5. The surface layer microstructure after WEDM (LM); magnification rate: 20x.

Regardless of the material, all spark-eroded surfaces exhibit a recast layer, which adheres to them to a certain extent, depending on the conditions; such a layer forms due to the local impact of the high temperatures accompanying a discharge and causes the surface layer of the material being machined to melt, partially or in full. The thickness of the recast layer follows from the setting of the machine parameters [Newton 2009], [Puri 2005] and, more prominently, the actual material and the related thermal treatment.
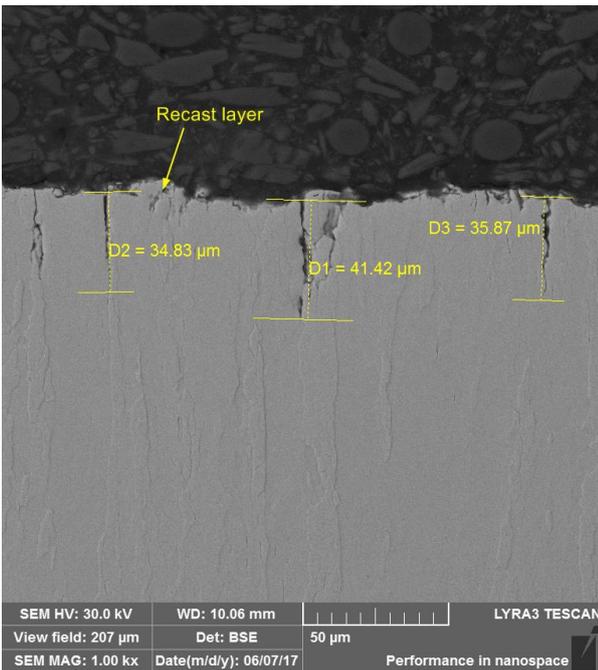
Figure 6. A cross section through the sample (SEM); magnification rate: 1,000x.

The cross section in Fig. 6 shows very long cracks (up to 41.42 µm) along the grain boundaries; these cracks are seen every 50 µm of the surface of the sample. The character of an exemplary crack is represented in Fig. 7.
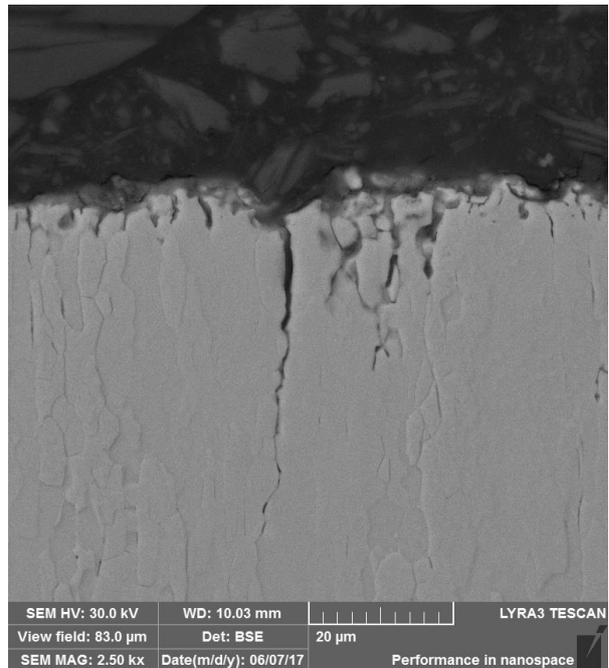
Figure 7. A cross section through the sample (SEM); magnification rate: 2,500x.

3.4 Hardness measurement

We employed the Hysitron TI 950 TriboIndenter nanoindenter with a Berkovich tip to investigate the workpiece hardness variation arising from the use of the WEMD technique. The load exerted on the sample by the tip during the measurement reached 6 mN. The twenty-four measured points were arranged into a 3x8 matrix (with the distance between the individual measurements corresponding to 18x10 µm), Fig. 8a.

Place of meas.	A (GPa)	B (GPa)	C (GPa)
1	4.611	4.505	4.665
2	4.777	4.795	4.354
3	4.920	4.790	4.351
4	4.522	5.015	4.357
5	4.572	4.749	4.394
6	4.502	4.603	4.258
7	4.324	4.511	4.175
8	4.963	4.289	4.658
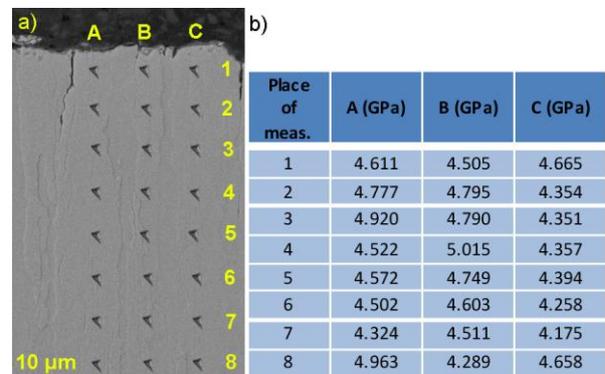
Figure 8. a) The individual hardness measurement spots; b) the measured values.

According to the data in Fig. 8b, the molybdenum did not exhibit a marked thermal impact on the layer; such an effect is nevertheless observable in, for example, iron-based materials [Lin 2005], where the hardening process enables the heat-affected layer to show higher local hardness values. The effect could not be detected in the molybdenum, because its melting temperature equals 2,623 °C, exceeding that of steel by 1,200 °C. The minor differences in the measured values can be ascribed to the specificity of the individual grain types.

4 CONCLUSION

The present paper focused on the problem of machining a welding electrode via the unconventional wire EDM cutting method. In the given context, the authors performed a detailed analysis of the experimental machined surface to yield the following results:

- the value of the surface quality parameter Ra, evaluated at five different locations, ranged between 2 and 2.7 μm;
- the inspection of the electrode morphology revealed long cracks having a width of up to 3 μm and scattered across the entire surface;
- the local chemical composition analysis disclosed that the basic material was only minimally contaminated with the elements of the wire electrode (max. 5.8 wt.% Cu and max 0.2 wt.% Zn);
- the metallographic specimens, or cross sections through the sample, exhibited cracks at the grain boundaries, reaching depths of up to 41 μm;
- the recast layer covers merely 5 % of the total surface of the machined sample, and its thickness does not exceed 5 μm;
- the triboindenter available was employed to measure the hardness at 24 points on the sample, with the results indicating that the subsurface layer of the sample had not been affected by the short-term exposure to high temperatures and that its hardness remained unchanged.

Based on the above summarization, it is possible to conclude that using the WEDM technique to machine pure molybdenum produces major cracks in the machined surfaces; such defects then may substantially affect the functionality, performance, and life cycle of relevant parts or components.

REFERENCES

[Aspinwall 2008] Aspinwall, D. K., Soo, S. L., Berrisford, A. E., & Walder, G. (2008). Workpiece surface roughness and integrity after WEDM of Ti–6Al–4V and Inconel 718 using minimum damage generator technology. *CIRP Annals-Manufacturing Technology*,*57*(1),pp.187-190.

[Blecha 2011a] Blecha, P., Blecha, R., Bradac, F. (2011). Integration of Risk Management into the Machinery Design Process. In Mechatronics Springer Berlin Heidelberg, pp. 473-482.

[Blecha 2011b] Blecha, P., & Prostrednik, D. (2011). Influence on the failure probability. Annals of DAAAM & Proceedings, pp. 11-13.

[Harcarik 2016] Harcarik, M., & Jankovych, R. (2016) Relationship Between Values of Profile and a real Surface Texture Parameters. MM Science Journal, 5, pp. 1659-1662. DOI: 10.17973/MMSJ.2016_12_2016206.

[Hasson 1968] Hasson, R. (1968). Metallography of molybdenum in color. Microscope, 16, pp. 329-334.

[ISO 25178-2] Geometrical Product Specifications (GPS) -Surface texture: Areal -Part 2: Terms, definitions and surface texture parameters. ISO 25178-2 (2012). Geneva: International Organization for Standardization.

[ISO 4287] Geometrical Product Specifications (GPS) -Surface texture: Profile method -Terms, definitions and surface texture parameters. ISO 4287 (1997). Geneva: International Organization for Standardization.

[Jiang 2012] Jiang, X. J., & Whitehouse, D. J. (2012). Technological shifts in surface metrology. CIRP Annals-Manufacturing Technology, 61(2), pp. 815-836.

[Kumar 2013] Kumar, A., Kumar, V., & Kumar, J. (2013). Experimental Investigation on material transfer mechanism in WEDM of pure titanium (Grade-2). Advances in Materials Science and Engineering.

[Lin 2005] Lin, H. C., Lin, K. M., Chen, Y. S., & Chu, C. L. (2005). The wire electro-discharge machining characteristics of Fe–30Mn–6Si and Fe–30Mn–6Si–5Cr shape memory alloys. Journal of materials processing technology, 161(3), pp. 435-439.

[Maher 2015] Maher, I., Sarhan, A. A., & Hamdi, M. (2015). Review of improvements in wire electrode properties for longer working time and utilization in wire EDM machining. The International Journal of Advanced Manufacturing Technology, 76(1-4), pp. 329-351.

[Mandal 2014] Mandal, A., & Dixit, A. R. (2014). State of art in wire electrical discharge machining process and performance. International Journal of Machining and Machinability of Materials, 16(1), pp. 1-21.

[McGeough 1988] McGeough, J. A. (1988). Advanced methods of machining. Springer Science & Business Media, ISBN 9780412319709.

[Mouralova 2017] Mouralova, K., Kovar, J., Klakurkova, L., Prokes, T., & Horynova, M. (2017). Comparison of morphology and topography of surfaces of WEDM machined structural materials. Measurement, 104, 12-20.

[Newton 2009] Newton, T. R., Melkote, S. N., Watkins, T. R., Trejo, R. M., & Reister, L. (2009). Investigation of the effect of process parameters on the formation and characteristics of recast layer in wire-EDM of Inconel 718. Materials Science and Engineering, pp. 208-215.

[Patel 2013] Patel, V. D., & Vaghmare, R. V. (2013). A review of recent work in wire electrical discharge machining (WEDM). International Journal of Engineering Research and Applications, 3(3), pp. 805.

[Puri 2005] Puri, A. B., & Bhattacharyya, B. (2005). Modeling and analysis of white layer depth in a wire-cut EDM process through response surface methodology. The International Journal of Advanced Manufacturing Technology, 25(3), pp. 301-307.

[Waikar 2008] Waikar, R. A., & Guo, Y. B. (2008). A comprehensive characterization of 3D surface topography induced by hard turning versus grinding. journal of materials processing technology, 197(1), pp. 189-199.

CONTACT:

Ing. Katerina Mouralova, Ph.D.
Brno University of Technology
Faculty of Mechanical Engineering
Technicka 2896/2, 616 69 Brno, Czech Republic
e-mail:mouralova@fme.vutbr.cz